# Specific Membrane Binding of Neurotoxin II Can Facilitate Its Delivery to Acetylcholine Receptor

Dmitry M. Lesovoy,[†] Eduard V. Bocharov,[†] Ekaterina N. Lyukmanova,[‡] Yurij A. Kosinsky,[†] Mikhail A. Shulepko,[‡] Dmitry A. Dolgikh,[‡] Mikhail P. Kirpichnikov,[‡] Roman G. Efremov,[†*] and Alexander S. Arseniev[†*]
[†]Division of Structural Biology and [‡]Division of Protein Engineering, Shemyakin-Ovchinnikov Institute of Bioorganic Chemistry RAS, Moscow, Russia

ABSTRACT The action of three-finger snake $\alpha$-neurotoxins at their targets, nicotinic acetylcholine receptors (nAChR), is widely studied because of its biological and pharmacological relevance. Most such studies deal only with ligands and receptor models; however, for many ligand/receptor systems the membrane environment may affect ligand binding. In this work we focused on binding of short-chain $\alpha$-neurotoxin II (NTII) from *Naja oxiana* to the native-like lipid bilayer, and the possible role played by the membrane in delivering the toxin to nAChR. Experimental (NMR and mutagenesis) and molecular modeling (molecular-dynamics simulation) studies revealed a specific interaction of the toxin molecule with the phosphatidylserine headgroup of lipids, resulting in the proper topology of NTII on lipid bilayers favoring the attack of nAChR. Analysis of short-chain $\alpha$-neurotoxins showed that most of them possess a high positive charge and sequence homology in the lipid-binding motif of NTII, implying that interaction with the membrane surrounding nAChR may be common for the toxin family.

## INTRODUCTION

Interactions between ligands and membrane receptors play a key role in many biological processes. One of the most intensively studied ligand/receptor systems is that of neurotoxins and nicotinic acetylcholine receptors (nAChRs), which are nonselective cation channels that mediate fast chemical transmission of electrical signal in the nervous system (1,2). The pentameric extracellular domain of nAChR contains ligand-binding sites for agonists (e.g., acetylcholine and nicotine) and antagonists (e.g., snake and cone snail toxins). Snake $\alpha$-neurotoxins are particularly interesting because of their different binding kinetics and the high affinity and selectivity of their interaction with various types of nAChRs, which are subdivided into two major classes—neuronal and muscle—depending on their localization and subunit composition. These toxins are small and stable proteins that retain their intrinsic ''three-finger'' $\beta$-structural fold upon binding to nAChR (1,3). Short-chain $\alpha$-neurotoxins (four disulfide bonds, 60–62 amino acid residues) selectively inhibit only muscle-type nAChRs, whereas long-chain $\alpha$-neurotoxins (five disulfide bonds, 66–75 amino acid residues) with an additional disulfide bond in the tip of the central loop (loop II) can inhibit both muscle and neuronal nAChRs (1,2). Although binding of $\alpha$-neurotoxins to nAChR has been extensively investigated with the aid of site-directed mutagenesis, chemical modifications, NMR, x-ray, and molecular modeling analyses in various studies (1,4–7), most of these studies focused on molecular models of the toxin-receptor complex formation, in which the membrane environment of nAChR was not taken into consideration.

However, it was found that for many membrane receptors, the lipid membrane could influence local concentration, diffusion, conformation, and orientation of a ligand, facilitating its recognition by the receptor, i.e., the membrane could optimize the ligand/receptor interaction through several different effects via the so-called ''membrane catalysis'' (also known as the ''membrane-compartment'') mechanism (8,9). In the case of nAChR, it is well known that some membrane properties (i.e., fluidity, surface charge density, lipid packing, and composition) affect functioning of the receptor and can influence its ligand binding (10–16). In particular, it was proposed that an approach of $\alpha$-neurotoxins to their binding sites is sensitive to the physical state of the plasma membrane surrounding nAChR (13). Thus, the lipid bilayer may play a certain role in $\alpha$-neurotoxin inhibition of nAChR. Notably, mammalian prototoxin lynx1, an endogenous nAChR modulator with the snake toxin-like fold, is normally presented at the cell surface as a glycophosphatidylinositol-anchored protein (17). Furthermore, the recently determined low-resolution (~14 Å) x-ray structure of $\alpha$-bungarotoxin (a long-chain $\alpha$-neurotoxin) in complex with the membrane-bound *Torpedo* nAChR revealed direct contacts between the toxin and the lipid bilayer surrounding the receptor (18). These facts prompted us to conduct a detailed investigation of the interaction between $\alpha$-neurotoxins and the membrane environment of nAChRs.

In this study we focused on the interaction of neurotoxin II (NTII), a short-chain $\alpha$-neurotoxin from *Naja oxiana*, with liposomes mimicking the membranes of native *Torpedo* nAChR, using the methods of NMR spectroscopy supported by mutagenesis and molecular modeling. A bacterial expression system developed for NTII (4) allowed the employment

*Submitted April 5, 2009, and accepted for publication July 24, 2009.*

Dmitry M. Lesovoy and Eduard V. Bocharov contributed equally to this work.

*Correspondence: efremov@nmr.ru or aars@nmr.ru

Editor: J. Antoinette Killian.



0006-3495/09/10/2089/9 $2.00

doi: 10.1016/j.bpj.2009.07.037

of heteronuclear NMR techniques. Previously, using this bacterial expression system the complex of $^{15}N/^{13}C$-labaled NTII with nAChR was characterized by solid-state NMR approach (3). Here we described the NTII membrane-binding site, which is remote from the receptor inhibition site and defines the position of a toxin molecule on the membrane surface in an orientation favoring subsequent docking to nAChR. Our findings are in agreement with the ''membrane catalysis'' concept, and indicate that the specific membrane binding of the toxin can precede receptor recognition, shedding new light on events that may occur during action of the $\alpha$-neurotoxins at their targets.

## MATERIALS AND METHODS

### Bacterial expression, isolation, and purification of recombinant NTII, its mutant, and $^{15}N$-labeled analogs

Recombinant NTII, its mutants, and their $^{15}N$-labeled analogs were produced as previously described (4). The mutations were introduced into the NTII gene by polymerase chain reaction on the basis of the previously developed plasmid pET22b/STII/NTII (4). The protocol used for the production and purification of uniformly $^{15}N$-labeled NTII and mutants was the same as for the nonlabeled toxins, with the exception that $^{15}NH_4Cl$ was used as the sole source of nitrogen ($^{15}N > 99\%$; Martek Biosciences, Columbia, MD). All steps for protein production, isolation, and purification were controlled by 12% Tris/Tricine sodium dodecyl sulfate polyacrylamide gel electrophoresis. The purity of the toxins was checked by analytical high-performance liquid chromatography (Smartline; Knauer, Berlin, Germany), which revealed the content of impurities as <5%. The N-terminal amino acid sequence of the obtained proteins was determined using a gas-phase sequenator (Protein Sequencer 470A; Applied Biosystems, Foster City, CA). Recombinant neurotoxins were analyzed by matrix-assisted laser desorption/ionization mass-spectrometry (Daltonics Ultraflex II TOF/TOF instrument; Bruker Daltonik, Bremen, Germany), circular dichroism (CD, J-810 spectropolarimeter; Jasco, Tokyo, Japan), and NMR spectroscopy.

### Liposome preparation

Synthetic membrane components—dioleoylphosphatidylcholine (DOPC), dioleoylphosphatidylserine (DOPS), and cholesterol (Chol)—were purchased from Avanti Polar Lipids (Alabaster, AL). A lipid composition of molar ratio DOPC/DOPS/Chol = 3:1:1 was prepared by mixing the phospholipids and cholesterol dissolved in chloroform/methanol (volume ratio 2:1), and evaporation on a SpeedVac vacuum dryer (Savant, Waltham, Quebec, Canada) followed by overnight drying at high vacuum. Multilamellar bilayer liposomes were prepared by dissolving lipid powders in 10 mM NaOAc buffer, pH 5.5, containing 5% $^2H_2O$, 1 mM EDTA, and 1.5 mM KCl. Freeze-thawing and mechanical agitation for 2 h were performed to facilitate hydration of the lipids. Monolamellar liposomes were prepared by extruding a multilamellar liposome dispersion through a polycarbonate filter with a pore size of 1000 Å using an Avanti Mini-Extruder. The recombinant NTII dissolved in the same buffer was added to the liposomes to obtain the required lipid/toxin ratio. Thermocycling and thorough stirring were used as described previously (19) to homogenize the samples containing NTII and liposomes.

### Acquisition and analysis of NMR spectra

All NMR experiments were performed on liquid crystalline bilayer membranes at 303 K. The $^{31}P$-NMR spectra were obtained on a DRX-500 spectrometer (Bruker BioSpin, Rheinstetten, Germany) with the aid of a spin-echo sequence as described previously (19), with an interpulse delay of 40 $\mu$s and repetition time of 3–5 s. Typically, 8192–57344 scans were acquired. Symmetrical 5 mm/15 mm NMR tubes (Shigemi, Allison Park, PA) were used. During acquisition, broadband $^1H$ decoupling was applied. Spectral processing was performed with the TOPSPIN software (Bruker BioSpin). Theoretical $^{31}P$-NMR spectra were calculated and fitted to the experimental ones using the P-FIT program under the assumption that in a magnetic field the liposomes will adopt an ellipsoidal shape (20). The adjustable parameters of the fit were the chemical shift anisotropies (CSAs), integral intensities, axis ratio of the ellipsoidal liposomes ($c/a$), and broadening function parameters. The $^1H$ WATERGATE (21) and $^1H$-$^{15}N$ heteronuclear single quantum coherence (HSQC) (22) spectra for free NTII or NTII/liposome suspension samples were acquired on a Unity-600 spectrometer (Varian, Palo Alto, CA) using standard 5 mm NMR tubes. $^1H$-$^{15}N$ HSQC spectra were detected as previously described (22), with an acquisition time $t_2$ of 0.1 s, 1600 data points, relaxation delay of 1.9 s, typically 32 scans, and 100 complex $t_1$ increments. Spectral widths were 1800 Hz in $F_1$ and 8000 Hz in $F_2$. The nitrogen decoupling during acquisition was achieved through the use of a 1 kHz WALTZ decoupling field as previously described (22). Assignment of the $^1H$ and $^{15}N$ resonances of NTII was taken from Bocharov et al. (23). NMR spectra were analyzed using the VNMR (Varian, Palo Alto, CA) program. The sensitivity of the NMR probe was monitored using the $^1H$-NMR signal of the NaOAc buffer contained in the samples. Crosspeak amplitude analysis in the set of $^1H$-$^{15}N$ HSQC spectra acquired at KCl titration of the NTII/liposome samples was performed with the Mathematica program (Wolfram Research, Champaign, IL).

### Molecular-dynamics simulation of NTII/membrane interaction

The molecular dynamics (MD) of the system containing NTII (Protein Data Bank entry 1NOR) and hydrated explicit lipid bilayer of 128 DOPS molecules was simulated using the GROMOS96 force field and GROMACS software (24). The construction of the protein/lipid system and the MD protocol are described in the Supporting Material. Two independent 6-ns MD runs were performed. In both cases, the molecule of NTII was initially placed at ~5 Å (~15 Å for toxin center of mass) above the membrane surface (defined as the average position of the phosphorous atoms of lipids in the nearest monolayer). Furthermore, the starting system configurations had different NTII orientations, with the head region of NTII positioned close to the membrane (see Fig. 2 *C*).

## RESULTS

### NTII binds strongly to the lipid bilayer mimicking the nAChR membrane environment

Native nAChR membranes are composed of phospholipids (~70%) with zwitterionic (mainly phosphatidylcholine and phosphatidylethanolamine) and anionic (mainly phosphatidylserine, as well as phosphatidylinositol, cardiolipin, and phosphatidic acid) headgroups, and cholesterol (~20%). The fraction of anionic phospholipids varies from ~25% on average for native nAChR membranes up to ~45% for nAChR-vicinal lipids (12,25). Experiments with nAChR embedded in model lipid membranes have shown that the functional conformations of nAChR and their changes upon ligand binding are quite sensitive to the membrane composition, i.e., to cholesterol, phosphatidylserine, and some zwitterionic phospholipids such as phosphatidylcholine and phosphatidylethanolamine (11,12,14). In particular, nAChR retains functional activity in a model lipid bilayer

composed of phosphatidylcholine, phosphatidylserine, and cholesterol with a molar ratio of 3:1:1 (11,14).

Therefore, we chose the membrane composition DOPC/DOPS/Chol = 3:1:1, which mimics the native-like membrane environment of nAChR, to uncover a possible role of the cell membrane in receptor/NTII interactions. Preliminary experiments showed a strong interaction of NTII with the membrane up to the sample precipitation under low ionic strength. To determine the lipid/protein molar ratio (L/P) at which NTII is completely bound to the membrane, $^{1}$H-NMR spectra of NTII in aqueous solution were monitored in the presence of an increasing amount of DOPC/DOPS/Chol liposomes in a liquid-crystalline state. The increase of lipid concentration resulted in attenuation of the NMR signal amplitudes of the toxin until their disappearance due to complete binding and immobilization of NTII on the lipid bilayer at L/P ~40:1 under 30 mM KCl (Fig. 1 *A*). In addition, the NTII binding to both pure DOPC and DOPS membranes was analyzed under the same conditions. It was found that NTII binds to the anionic DOPS bilayer (full binding at L/P ~6:1) (Fig. 1 *B*) but does not bind to the zwitterionic DOPC bilayer (data not shown).

Finally, it was found that under physiological ionic strengths of ~150 mM, immobilization of 1 mM NTII was achieved at lipid concentrations >~140 mM (Fig. S1 *A*) and ~70 mM (Fig. S1 *B*) for anionic lipid fractions of 25% and 45%, respectively. This effect is a consequence of the weakening of electrostatic attraction between the cationic protein and the negatively charged membrane with the increasing ionic strength. Overall, the anionic lipid fraction, L/P molar ratio, and ionic strength of the solution shift the equilibrium of the NTII binding to the lipid bilayer mimicking the nAChR membrane environment. The effective lipid concentration in the synaptic cleft is >200 mM, as estimated from the characteristic synaptic cleft width (~200 Å) and mean area per one lipid in the bilayer (~64 Å$^2$). Thus, even at physiological ionic strength, most of the toxin molecules should be bound to the lipid bilayer surrounding nAChR due to the high fraction of anionic lipids and the large effective lipid concentration in vivo.

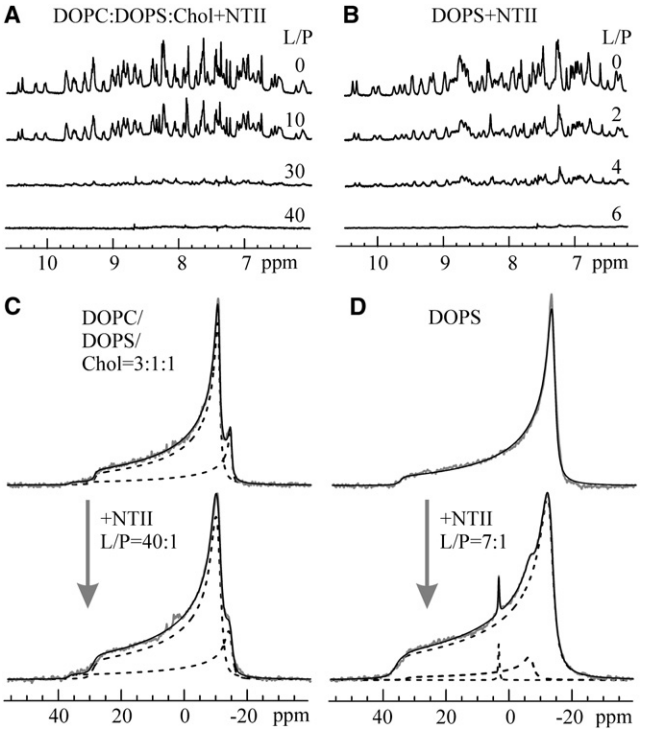


FIGURE 1 NTII binding to lipid bilayers mimicking the nAChR membrane environment. (*A* and *B*) $^{1}$H-NMR spectra of 0.3 mM NTII in the presence of DOPC/DOPS/Chol = 3:1:1 (*A*) and DOPS (*B*) liposomes, 30 mM KCl, 10 mM NaOAc, pH 5.5, 303 K. The lipid/protein (L/P) molar ratio is indicated on the right of each spectrum. Membrane perturbations upon NTII binding are shown. (*C* and *D*) $^{31}$P-NMR spectra of a total 26 mM concentration of DOPC/DOPS/Chol = 3:1:1 (*C*) and 20 mM DOPS (*D*) multilamellar liposomes, 30 mM KCl, 10 mM NaOAc, pH 5.5, 303 K without and with membrane-bound NTII. Experimental spectra, theoretical approximation, and lineshape decomposition are indicated by gray, black, and dashed lines, respectively. The parameters of $^{31}$P-CSA for DOPC and DOPS, liposome deformation ($c/a$) in the magnetic field, and relative intensities of DOPC and DOPS signals were estimated to be, respectively, (*C*) without NTII: 39 ± 1 ppm and 51 ± 1 ppm, 1.21 ± 0.05, 75% and 25%; with NTII: 40 ± 1 ppm and 51 ± 1 ppm, 1.15 ± 0.05, 75% and 25%; (*D*) without NTII: 50 ± 1 ppm, 1.34 ± 0.05, 100%; and with NTII: 50 ± 1 ppm, 31 ± 1 ppm and 0 ppm (isotropic phase), 1.13 ± 0.05, 86%, 13%, and <1%.

## NTII interacts only with the membrane surface and "captures" the headgroup of one DOPS molecule

Protein/membrane interactions may affect the physical properties of the lipid bilayer and the behavior of its components, which can be investigated with the aid of wide-line $^{31}$P-NMR spectroscopy. $^{31}$P-CSA is sensitive to alterations in the orientation and motion of lipid headgroups (26–28). Studies of NTII binding to multilamellar DOPC/DOPS/Chol and pure anionic DOPS liposomes (Fig. 1, *C* and *D*) revealed changes in $^{31}$P-CSA for the portion of DOPS molecules for both membrane compositions. This effect is more pronounced in the case of pure DOPS membrane, for which a typical "bilayer-like" $^{31}$P-NMR spectrum (Fig. 1 *D*) with $^{31}$P-CSA = 50 ppm was observed, whereas the NTII binding to the membrane leads to the appearance of an additional spectral component with reduced $^{31}$P-CSA (31 ppm; Fig. 1 *D*). The integral intensities of this additional component are ~13% and ~7% at a DOPS/NTII molar ratio of 7:1 and 14:1, respectively. This indicates that binding of one NTII molecule results in changes of orientation and/or motion of the headgroup in one DOPS molecule, which is involved in a specific interaction with neurotoxin. Unfortunately, in the case of mixed membrane, the analysis of an additional (NTII-induced) $^{31}$P-spectral component of DOPS was complicated by its overlapping with the prevailing (75%) signal from DOPC (Fig. 1 *C*) and large L/P ratio (40:1).

Due to the diamagnetic anisotropy of phospholipid molecules, multilamellar liposomes are stretched along the direction of the applied magnetic field (29) and adopt an

ellipsoidal shape. Protein binding and insertion may influence the membrane properties and alter the extent of liposome deformation in the magnetic field. This effect is manifested as a redistribution of the intensities between high- and low-field shoulders in a $^{31}$P-NMR spectrum (19,20). Analysis of the obtained $^{31}$P-NMR spectra shows that NTII binding to the multilamellar DOPC/DOPS/Chol liposomes (L/P = 40:1) leads to a slight reduction of the ellipsoid axes ratio ($c/a$) from 1.21 to 1.15 (Fig. 1 *C*). Similarly, NTII binding to a pure anionic DOPS bilayer (L/P = 7:1) results in a $c/a$ reduction from 1.34 to 1.13 (Fig. 1 *D*). We previously observed an analogous effect in cytotoxins, which are structural homologs of $\alpha$-neurotoxins from snake venom (19,30). However, in the case of cytotoxins, this effect was much greater—up to complete suppression of the liposome deformation ($c/a = 1$). Cytotoxins interact with lipid membrane, immersing slightly into its hydrophobic region. This leads to perturbation of the bilayer packing up to prevailing of nonbilayer lipid phase giving the isotropic $^{31}$P-signal near 0 ppm (26,27) with the signal intensity of up to 80% at L/P ~12 (19,30), whereas NTII binding results in a <1% formation of a nonbilayer (isotropic) lipid phase even at L/P = 7:1 (Fig. 1 *D*). Thus, the $^{31}$P-NMR data indicate that in contrast to cytotoxins, NTII does not significantly perturb the lipid bilayer packing, which is in good agreement with subsequent data indicating shallow insertion of the toxin into the membrane, no deeper than the lipid headgroups.

## Membrane-binding site of NTII is located in its "head" region

For a protein bound to a lipid bilayer (such as liposomes), the values of the rotational correlation time, and thus the NMR transverse relaxation rate, are much greater than in solution. Therefore, NMR signals of the NTII molecule in its membrane-bound state are broadened beyond detection. Nevertheless, it has been theoretically and experimentally shown that under certain conditions of slow and intermediate (on the NMR timescale) exchange between the free and bound states, the NMR spectra of a free-state protein are highly sensitive to chemical shift perturbations upon binding (so-called ''differential line-broadening'', e.g., as manifested in the differential reduction of crosspeak amplitudes in $^{1}$H-$^{15}$N HSQC spectra; see the Supporting Material) (31,32). To employ this ''differential amplitude reduction'' technique, we chose the experimental conditions so as to obtain an appreciable exchange rate and free/bound state ratio, as well as to be appropriate for high-resolution NMR spectroscopy (0.4 mM NTII, lipid/NTII = 40:1 and ~70 mM KCl).

The crosspeak amplitudes in the $^{1}$H-$^{15}$N HSQC spectra of the $^{15}$N-labeled NTII were monitored in the presence of monolamellar DOPC/DOPS/Chol liposomes as a function of KCl concentration. The results revealed a sigmoid-like growth of $^{1}$H$^{15}$N crosspeak amplitudes as a function of increasing salt concentration (Fig. 2 *A*). In the 30–120 mM range of KCl concentration, the toxin undergoes an appreciable exchange between free and membrane-bound states (an example of HSQC spectra is presented in Fig. S5 *B*). The $^{1}$H$^{15}$N crosspeak amplitude growth reached a plateau at KCl concentrations exceeding ~200 mM KCl, indicating the disappearance of the membrane-bound state. Of importance, the detailed analysis of the relative $^{1}$H$^{15}$N amplitudes growing near the flex point of the titration curve observed in three independent experiments permits subdivision of the NTII residues into two distinct groups (Fig. 2 *A*). It should be noted that the amplitude dispersion inside both groups coincides with the overall dispersion of $^{1}$H$^{15}$N crosspeak amplitudes during salt titration of the NTII sample without membranes (see Fig. S7). The minor group (Glu-2, Cys-3, Gln-6, Cys-17, Asn-22, Gly-41, Asn-50, and Arg-58 residues; Fig. 2 *F*) with decreased $^{1}$H$^{15}$N crosspeak amplitudes (Fig. 2 *B*) consists of amino acid residues whose $^{1}$H$^{15}$N chemical shifts undergo the greatest change upon NTII binding to the lipid bilayer.

The chemical shift changes could be a result of either a specific interaction of lipid molecules with their corresponding NH groups, or their chemical-shift hypersensitivity to environment perturbations upon NTII binding to the anionic bilayer. We investigated the latter possibility in several experiments by considering the ''hypersensitivity'' of chemical shifts of NTII $^{1}$H$^{15}$N crosspeaks to pH, dielectric constant, or KCl concentration (see the Supporting Material). These additional considerations did not reveal a prominent sensitivity of NH groups of Glu-2, Cys-3, Gln-6, Cys-17, Asn-22, Gly-41, and Arg-58 residues, whereas NH groups of Asn-50 showed a chemical-shift hypersensitivity to dielectric constant changes of the media. Therefore, Asn-50 cannot serve as an unambiguous probe of the NTII topology on the membrane. In turn, the spatial localization of Glu-2, Cys-3, Gln-6, Cys-17, Asn-22, Gly-41, and Arg-58 residues in the disulfide-rich ''head'' region of NTII obviously maps the membrane-binding site on the toxin surface (Fig. 2 *C*), which retains its overall structure upon binding (see the Supporting Material). Of importance, the mapped membrane-binding site is remote from the receptor inhibition site located on the tip of the central loop II of NTII, being at a distance up to 40 Å as estimated for side-chain atoms, and implying an independence of the membrane- and receptor-binding sites for NTII.

## MD simulations of NTII on the water-lipid interface decipher its membrane-bound topology

To obtain additional insights into the details of NTII/membrane interaction, we conducted an MD simulation study using an explicitly hydrated lipid bilayer. In both 6-ns MD runs, the toxin spontaneously moved closer to the bilayer surface and interacted with lipid headgroups. The time-dependent disposition of the NTII molecule on the membrane was quite variable. Nevertheless, a specific and stable interaction between NTII and the membrane was observed in one of the

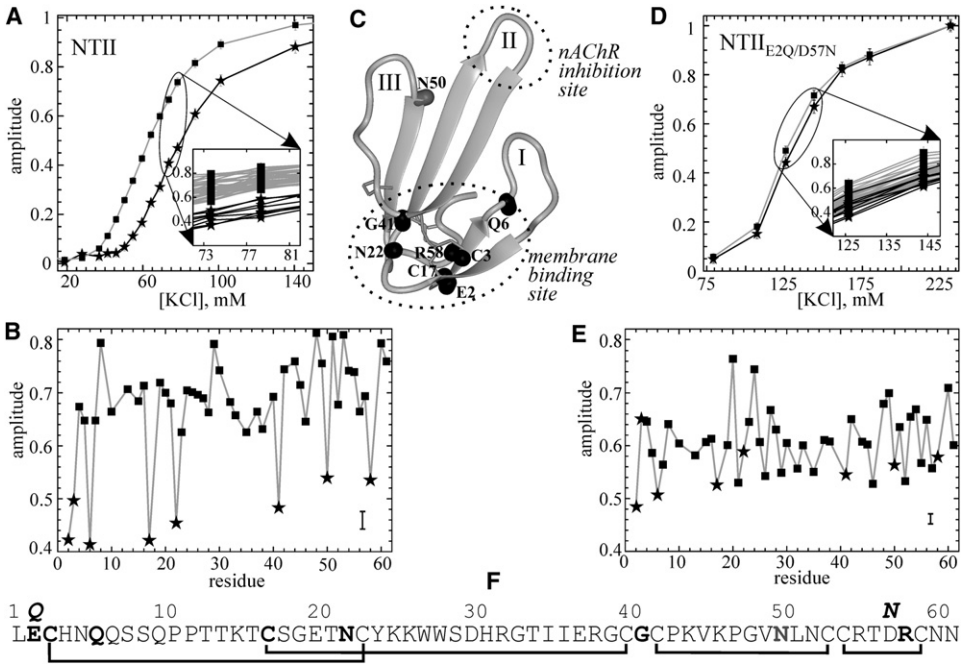


FIGURE 2 Residue-wise specificity of NTII interaction with the native-like nAChR membrane. (*A* and *D*) KCl concentration dependence of the cross-peak amplitudes in the $^{1}H$-$^{15}N$ HSQC spectra of 0.4 mM NTII and double mutant NTII$_{E2Q/D57N}$ in the presence of monolamellar DOPC/DOPS/Chol = 3:1:1 liposomes, L/P = 40:1. The amplitudes of the $^{1}H^{15}N$ crosspeaks were normalized to the corresponding amplitudes at 200 and 240 mM KCl when NTII and NTII$_{E2Q/D57N}$, respectively, were in the unbound state. The experimental sigmoid-like dependences averaged over residues without and with differential amplitude reduction are shown by boxes linked by gray lines and asterisks linked by black lines, respectively. (*Inset*) The behavior of all $^{1}H^{15}N$ crosspeak amplitudes near the flex point of titration curve is shown. Two groups of curves without (total mass) and with (eight curves) differential amplitude reduction are denoted as in the main panel. (*B* and *E*) The $^{1}H^{15}N$ crosspeak amplitudes of NTII and NTII$_{E2Q/D57N}$ were averaged over the 72–82 mM and 120–150 mM KCl range, respectively, and plotted against the residue number. The eight residues (Glu-2, Cys-3, Gln-6, Cys-17, Asn-22, Gly-41, Asn-50, and Arg-58) marked by asterisks clearly demonstrate differential amplitude reduction in the case of NTII; however, no pronounced differential amplitude reduction was observed for the NTII$_{E2Q/D57N}$ mutant. (*C*) Localization of the backbone HN groups of Glu-2, Cys-3, Gln-6, Cys-17, Asn-22, Gly-41, Asn-50, and Arg-58 (highlighted by *black balls*) in the NTII spatial structure presented by the ribbon diagram. The ''fingers'' of the toxin molecule are indicated by roman numerals. The mapped membrane-binding site and nAChR inhibition site are enclosed by dotted ovals. (*F*) The amino acid sequence of NTII. The residues that demonstrate differential amplitude reduction are highlighted in boldface. The residue numbers and amino acid substitutions are shown above the sequences. S-S bonds are displayed in black lines below the sequence.

simulations, which allowed identification of a particular topology of NTII molecule on the membrane. During the first ns of MD, the toxin approached the bilayer surface and finally settled in the lipid headgroup region, as shown in Fig. 3 *A*. This specific topology was retained during the remaining 5 ns of the simulation time. Analysis of the MD trajectories revealed that NTII formed the most stable contacts with a single DOPS molecule—its polar headgroup interacts with the charged side chains of Glu-2, Asp-57, and Arg-58, which are located exactly in the NTII membrane-binding site described above. The surface of the site possesses particular electrostatic properties (Fig. 3 *C*), i.e., there are regions of high negative and positive electrostatic potentials placed close to each other. Thus, the negatively charged phosphate and carboxyl groups of the DOPS molecule interact with the positively charged guanidine group of Arg-58, forming one to three hydrogen bonds, whereas the positively charged amino group of DOPS interacts with the carboxyl groups of Glu-2 and Asp-57, forming two hydrogen bonds (Fig. 3 *B* and Fig. S8). Two additional DOPS molecules that interacted occasionally with side chains of Glu-2, Thr-14, Thr-16, and Ser-18 were also identified (Fig. S9). To sum up, a variable network of intermolecular hydrogen bonds that forms upon the peripheral membrane binding of NTII constrains the orientational freedom of the toxin molecule ($30^\circ < \alpha < 60^\circ$, as denoted in Fig. 3 *A*), thus providing a specific but movable topology of the toxin on the membrane surface. Therefore, NTII/membrane interactions are flexible but not strong, in accordance with the sensitivity of the binding to ionic strength.

It should be mentioned that such an NTII topology on a lipid bilayer (Fig. 3 *A*) agrees well with experimental NMR data that map the membrane-binding site of NTII in its ''head'' region (Fig. 2 *C*). Also, for the most dense packing of NTII on the DOPS bilayer (at L/P = 6:1; Fig. 1 *B*), one of two possible orientations of NTII coincides with its orientation in MD (Fig. 3 *A*). Indeed, the maximal occupied area of the NTII molecule on a plane is ~860 Å$^2$ (in the loop plane) and the minimal one is ~380 Å$^2$ (perpendicular to the loop II direction). The area of six DOPS molecules on a lipid bilayer is ~390 Å$^2$ (33); thus, the NTII molecule participating in saturating binding to a pure DOPS bilayer (as shown in the previous section) should be positioned with its loop II directed close to the bilayer normal (as in Fig. 3 *A*).

## Mutations in the NTII head region eliminate the specific toxin-membrane interaction

To confirm the importance of the toxin head region in the membrane binding, we substituted the identified NTII residues that participated during the MD simulation in

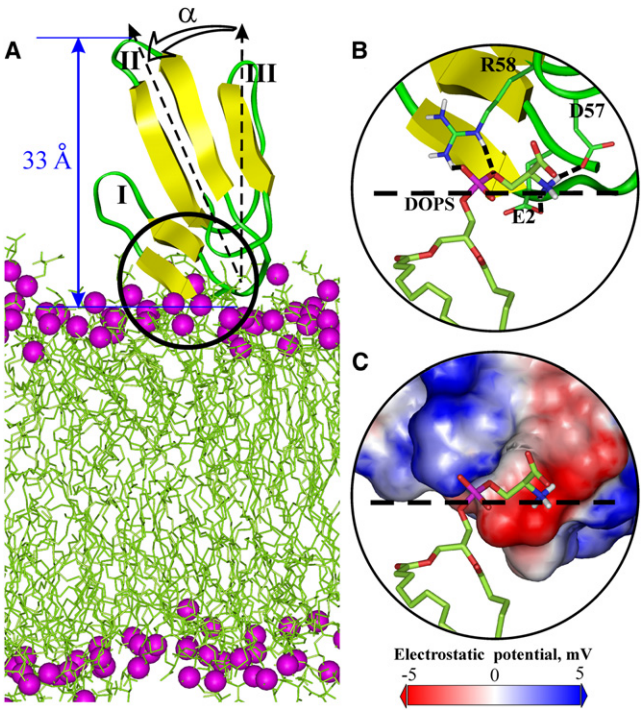


FIGURE 3 Topology of NTII on the membrane surface. (*A*) MD model of NTII association with an explicit DOPS bilayer. The angle $\alpha$ between the central loop of NTII (vector Thr-21 $C^{\alpha}$ –His-31 $C^{\alpha}$) and the membrane normal is shown. The distance between phosphorus atoms (*magenta balls*) of lipids and the top tip of the toxin loop II (nAChR inhibition site) is denoted by the blue arrow. (*B*) ''Capture'' of the lipid phosphatidylserine headgroup by the side chains of Glu-2, Asp-57, and Arg-58 from the NTII membrane-binding site. The toxin side chains and lipid molecule are shown in stick representation. The carbon, nitrogen, proton, oxygen, and phosphorus atoms of the toxin and lipid are colored in green, blue, white, red, and magenta, respectively. Intermolecular hydrogen bonds are indicated by dotted lines. The bilayer interface (average position of lipid headgroup phosphorus atoms) is depicted by the dashed line. (*C*) Electrostatic interaction of negatively charged phosphate and dipolar serine groups of DOPS with the NTII membrane-binding site, which is colored according to the surface electrostatic potential calculated using the DelPhi program (41).

the specific recognition of the DOPS headgroup. We engineered a double Glu-2Gln/Asp-57Asn-mutant of NTII ($NTII_{E2Q/D57N}$) for more effective elimination of hydrogen bonding with the DOPS lipid headgroups. CD and NMR spectra demonstrated that the folding was successful and the native toxin structure was preserved for $NTII_{E2Q/D57N}$ (Fig. S2 *B* and Fig. S4). We then studied the binding of the uniformly $^{15}N$-labeled $NTII_{E2Q/D57N}$ to the bilayer mimicking the nAChR membrane by NMR.

In a manner similar to that used for wild-type NTII, we monitored the crosspeak amplitudes in the $^{1}H$-$^{15}N$ HSQC spectra of $NTII_{E2Q/D57N}$ in the presence of monolamellar DOPC/DOPS/Chol liposomes at L/P = 40:1 as a function of KCl concentration (Fig. 2 *D*). In the ~80–220 mM range of KCl, the toxin undergoes an appreciable exchange between free and membrane-bound states, and the complete release of $NTII_{E2Q/D57N}$ from the liposome surface was achieved at ~240 mM KCl. The corresponding KCl concentrations were larger for $NTII_{E2Q/D57N}$ than for the native NTII due to the extra charge of +2 for the double mutant and hence the stronger electrostatic attraction of the mutant toxin molecule to the negatively charged membrane surface. In contrast to NTII, a detailed analysis of the crosspeak amplitudes near the flex point of the titration curve (~150 mM KCl) did not reveal a differential amplitude reduction and consequent selective chemical shift perturbations upon $NTII_{E2Q/D57N}$ membrane binding (Fig. 2 *E*). Also, binding of $NTII_{E2Q/D57N}$ to DOPC/DOPS/Chol and DOPS liposomes did not result in changes of $^{31}P$-CSA for DOPS molecules (data not shown), revealing the absence of specific interactions of $NTII_{E2Q/D57N}$ with DOPS molecules. Together, these findings imply the absence of a specific membrane-binding site for the $NTII_{E2Q/D57N}$ molecule, and hence the absence of a preferable orientation on the membrane. Note that our modeling and experimental (both NMR and mutagenesis) data correlate well in revealing a specific interaction of the NTII head region primarily with one DOPS molecule.

## DISCUSSION

### Specific interaction of NTII with the membrane surface can facilitate its receptor search and recognition

Using heteronuclear NMR and molecular modeling supported by mutagenesis, we showed that short-chain $\alpha$-neurotoxin NTII binds by its head region to the lipid bilayer mimicking the nAChR membrane environment (Fig. 2 *C*) without insertion into the hydrophobic core of the bilayer. The charged and hydrophilic side chains of NTII residues in the mapped membrane-binding site participate in formation of a labile net of hydrogen bonds with polar lipid headgroups, resulting in distinctive positioning of the toxin molecule relative to the membrane surface (Figs. 2 *C* and 3). In this orientation, the tip of the toxin loop II, which is responsible for nAChR inhibition, can be raised up to 30–35 Å (distance for backbone atoms) above the lipid headgroup region (Fig. 3 *A*). This is quite favorable for the attack of the receptor from the membrane-facing periphery, since the nAChR ligand-binding pocket locates no more than ~40 Å away from the membrane interface (1,12,18,34). Moreover, the peripheral membrane binding allows the toxin molecule to be sufficiently motile (Fig. 3 *A*) to be properly recognized by nAChR.

According to the so-called ''membrane catalysis'' concept (8,9), which is believed to be essential for many ligand/receptor systems, ligands recognize their targets in membrane-embedded receptors from the membrane-bound state, thereby accelerating the ligand search of the receptor and facilitating ligand docking to the receptor. Intermolecular contacts established during the membrane association and receptor recognition events can result in subsequent

conformational changes in both the ligand and receptor. The lipid-binding site of the ligand, which determines its topology on or in the membrane, is called the ''address'', and the part that contains residues directly involved in forming contacts to the receptor is identified as the ''message''. Often the sites are somewhat remote, and amino acid substitutions in the address region will not seriously affect the affinity to the receptor.

In the case of NTII, our findings are in agreement with the key feature of the ''membrane catalysis'' mechanism, namely, that the membrane promotes ligand accumulation in a movable optimized topology on the membrane surface favoring ligand-receptor recognition. Hence, the membrane binding can be considered as an initial event preceding nAChR recognition by NTII. According to the membrane-catalysis concept as applied to NTII action at nAChR, the positively charged toxin molecules are initially accumulated above or on the membrane surface due to its electrostatic potential (Fig. 4, step A→B). The immediate increase in the NTII concentration above the membrane is regulated by the content of negatively charged phospholipids in the lipid bilayer and the ionic strength of the solution. The subsequent specific binding of NTII to the lipids provides positioning of NTII on the lipid bilayer (Fig. 4, step B→C) in a location suitable for attack of the receptor (as discussed in detail above). Finally, the positioned NTII molecule diffuses laterally in the lipid-bound state to nAChR (Fig. 4, step C→nAChR), which may be advantageous depending on several different factors (8), including the membrane concentrations of the receptors. These steps can be partially directed and accelerated by an increase in the fraction of anionic phospholipids in the nAChR-vicinal lipid bilayer (12,25) and by the ability of nAChR to concentrate cations (34,35). Overall, these membrane-binding steps are rate limiting, and the reaction kinetics could be several orders of magnitude faster than for the ligand/receptor interaction without accumulation on the membrane (8,36).

The specific interaction of NTII with the membrane surface apparently gives rise mainly to a kinetic advantage for nAChR inhibition, but should not significantly influence the final ligand/receptor complex configuration. Thus, the membrane serves mainly to deliver the toxin molecule to nAChR in a proper orientation to facilitate receptor recognition by the toxin inhibition site located above the membrane surface on the same level with the nAChR ligand-binding pocket. This assumption is supported by available literature data that were obtained for short-chain $\alpha$-neurotoxins by means of competitive binding measurements, and demonstrate that amino acid substitutions in the toxin head region do not significantly affect the nAChR inhibition activity (37,38). Moreover, it is conceivable that the toxin would not interact simultaneously with the membrane and the receptor in the final NTII/nAChR complex, since the toxin binding into the receptor ligand-binding pocket is incommensurately stronger than its transitory interactions with lipid headgroups.

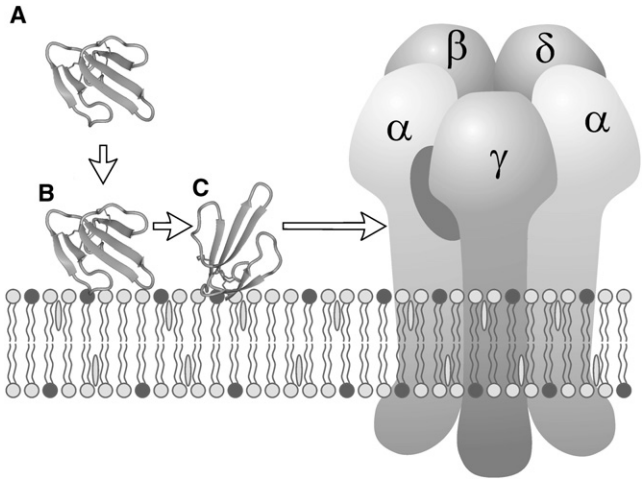


FIGURE 4 Membrane catalysis for the nAChR inhibition pathway of NTII. Step A→B: unspecific electrostatic adsorption of the positively charged toxin from solution to the negatively charged surface of a cell membrane. Step B→C: anchoring of the toxin to the lipid headgroups in a specific orientation that favors the receptor recognition. Step C→nAChR: NTII lateral diffusion and subsequent recognition of nAChR. The toxin-binding site between $\alpha$- and $\gamma$-subunits of nAChR is marked by a gray oval. NTII, nAChR, and lipid bilayer are shown schematically.

A previous low-resolution x-ray study (18) suggested that a long-chain $\alpha$-neurotoxin ($\alpha$-bungarotoxin) in the nAChR-bound state interacts with the phospholipid headgroups of the surrounding membrane, presumably by head and side loop regions of the toxin molecule. Such a configuration is in agreement with the recently obtained crystal structure of the extracellular domain of nAChR $\alpha$1 subunit bound to $\alpha$-bungarotoxin (7), as well as with modeling of the binding mode of $\alpha$-bungarotoxin to nAChR based on x-ray and NMR data (1,39). Although long- and short-chain $\alpha$-neurotoxins may differ in terms of both membrane- and receptor-binding topology, these data imply that the short-chain $\alpha$-neurotoxin NTII can maintain membrane contacts at least during initial recognition of the nAChR. It should be noted that earlier EPR and fluorescence studies mapped the head region of NTII as an additional site that participates in interaction with nAChR preparations (40). Also, it is interesting to note that an endogenous nAChR modulator lynx1, which adopts the three-fingered toxin fold characteristic of $\alpha$-neurotoxin, has a consensus C-terminal sequence, suggesting its attachment to the membrane surface via a glycophosphatidylinositol-anchor (17).

## Specific membrane binding may be widespread among the $\alpha$-neurotoxin family

There are many ''three-finger'' $\alpha$-neurotoxins of different origins that effectively inhibit nAChRs. Most of these neurotoxins possess a high positive charge (Fig. S10), which favors their electrostatic accumulation on the membrane surrounding nAChR. Therefore, it is reasonable to assume that membrane recognition could be quite common for

α-neurotoxins. Indeed, a comparison of a number of short-chain α-neurotoxins (Fig. S10, lines 1–14) shows a high level of homology for residues in positions 2, 57, and 58, which participate in specific interactions with the phosphatidylserine headgroup (Fig. 3, *B* and *C*), and in positions 15 and 20, which also form the electrostatic pattern of the membrane-binding site. As a result, the phosphatidylserine-binding motif of the toxins is formed by positively charged Arg or Lys residues in position 58, and negatively charged Asp and Glu residues in positions 2 and 57. In some short-chain α-neurotoxins, a coupled rearrangement of charged residues in the membrane-binding site occurs (Fig. S10, lines 23–25). Although some toxins reveal a lower level of homology in the membrane-binding site (Fig. S10, lines 15–22 and 26–30), overall these findings support the idea that membrane catalysis may contribute to the action of short-chain α-neurotoxins at nAChR.

Long-chain α-neurotoxins are also cationic proteins, and it has been proposed that they interact with the membrane surface in complex with nAChR (18). However, long α-neurotoxins do not demonstrate a sequence homology (Fig. S11) with short α-neurotoxins located along the identified membrane-binding site. Therefore, one can expect possible membrane interactions of long α-neurotoxins to differ from those revealed for short ones that (assuming the membrane-catalysis mechanism is correct) should affect receptor inhibition kinetics. This means that the specificity of the interaction of long-chain α-neurotoxins with membranes deserves further study.

## CONCLUSIONS

It seems logical to assume that for snake neurotoxins to evolutionarily achieve a highly specific receptor recognition system, they had to be able to use the entire range of different molecular mechanisms available to them. For many membrane receptors, the specific interactions of their ligands with membrane have been recognized as assisting in ligand binding (8,9); however, up to now, the role of the lipid environment in nAChR inhibition by snake α-neurotoxins has been disregarded. We have demonstrated a specific interaction of the short-chain α-neurotoxin NTII with nAChR native-like lipid bilayer via hydrogen bonding with the lipid headgroups. Such specific binding may facilitate toxin delivery and its association with the receptor via membrane catalysis. This is achieved by means of a local toxin concentration increase in the membrane-bound state, with a moveable topology suitable for receptor recognition that implies proper toxin orientation and position leveling of the toxin receptor-binding site relative to the nAChR ligand-binding pocket.

There may be a physiological explanation for the fact that under physiological conditions the α-neurotoxin binds to the membrane only at high values of effective anionic lipid concentration. Specifically, the toxin molecules that are transported through the blood and lymph vessels, where the effective lipid/toxin molar ratio is low, should not adsorb onto cell membranes; rather, they should interact with the cell surface in the narrow cleft between the nerve ending and the muscle fiber, where the effective concentration of the anionic lipids (in particular, phosphatidylserine) is high. In other words, the specific toxin-lipid interaction and the proposed membrane-catalysis mechanism should be activated only in the vicinity of postsynaptic membrane. Furthermore, the possible influence of the transmembrane potential on toxin binding to the postsynaptic membrane cannot be excluded.

Overall, these findings imply that the postsynaptic membrane is more than just a passive platform for integrating all participants in a signal transduction process through nAChR. Therefore, specific membrane properties in the vicinity of nAChR have to be taken into account in the development of actual models of toxin-receptor complexes, and pharmacologically relevant ligands of the receptors. Indeed, it was recently observed that local anesthetic actions at nAChR are sensitive to the lipid environment, in particular to a negative charge of the membrane surface (10).

Of course, the direct relation between the membrane-binding properties and biological activity of NTII requires further research, including a thorough investigation of the toxin-binding kinetics. We believe that our findings will stimulate new studies to elucidate the details of the molecular mechanisms that govern specific nAChR recognition by α-neurotoxins and other ligands, and particularly the role of the membrane environment in this process.

## SUPPORTING MATERIAL

Additional text, a table, 11 figures, and references are available at http://www.biophysj.org/biophysj/supplemental/S0006-3495(09)01302-2.

We thank V. I. Tsetlin, I. E. Kasheverov, and Z. O. Shenkarev for helpful discussions.

This work was supported by the Russian Foundation for Basic Research, the Russian Federal Agency of Science and Innovations, Russian Academy of Sciences (Program on Molecular and Cellular Biology), and a grant from the President of the Russian Federation (MK-6386.2008.4).

## REFERENCES

1. Dutertre, S., and R. J. Lewis. 2006. Toxin insights into nicotinic acetylcholine receptors. *Biochem. Pharmacol.* 72:661–670.
2. Fruchart-Gaillard, C., G. Mourier, C. Marquer, A. Menez, and D. Servent. 2006. How three-finger-fold toxins interact with various cholinergic receptors. *J. Mol. Neurosci.* 30:7–8.
3. Krabben, L., B. J. van Rossum, F. Castellani, E. Bocharov, A. A. Schulga, et al. 2004. Towards structure determination of neurotoxin II bound to nicotinic acetylcholine receptor: a solid-state NMR approach. *FEBS Lett.* 564:319–324.
4. Lyukmanova, E. N., Z. O. Shenkarev, A. A. Schulga, Y. S. Ermolyuk, D. Y. Mordvintsev, et al. 2007. Bacterial expression, NMR and electrophysiology analysis of chimeric short/long-chain α-neurotoxins acting on neuronal nicotinic receptors. *J. Biol. Chem.* 282:24784–24791.

5. Kessler, P., R. Thai, F. Beau, J. L. Tarride, and A. Menez. 2006. Photocrosslinking/label transfer: a key step in mapping short $\alpha$-neurotoxin binding site on nicotinic acetylcholine receptor. *Bioconjug. Chem.* 17:1482–1491.
6. Bourne, Y., T. T. Talley, S. B. Hansen, P. Taylor, and P. Marchot. 2005. Crystal structure of a Cbtx-AChBP complex reveals essential interactions between snake $\alpha$-neurotoxins and nicotinic receptors. *EMBO J.* 24:1512–1522.
7. Dellisanti, C. D., Y. Yao, J. C. Stroud, Z. Z. Wang, and L. Chen. 2007. Crystal structure of the extracellular domain of nAChR $\alpha$1 bound to $\alpha$-bungarotoxin at 1.94 A resolution. *Nat. Neurosci.* 10:953–962.
8. Castanho, M. A., and M. X. Fernandes. 2006. Lipid membrane-induced optimization for ligand-receptor docking: recent tools and insights for the ''membrane catalysis'' model. *Eur. Biophys. J.* 35:92–103.
9. Schwyzer, R. 1995. 100 years lock-and-key concept: are peptide keys shaped and guided to their receptors by the target cell membrane? *Biopolymers.* 37:5–16.
10. Baenziger, J. E., S. E. Ryan, M. M. Goodreid, N. Q. Vuong, R. M. Sturgeon, et al. 2008. Lipid composition alters drug action at the nicotinic acetylcholine receptor. *Mol. Pharmacol.* 73:880–890.
11. daCosta, C. J., I. D. Wagg, M. E. McKay, and J. E. Baenziger. 2004. Phosphatidic acid and phosphatidylserine have distinct structural and functional interactions with the nicotinic acetylcholine receptor. *J. Biol. Chem.* 279:14967–14974.
12. Barrantes, F. J. 2004. Structural basis for lipid modulation of nicotinic acetylcholine receptor function. *Brain Res. Brain Res. Rev.* 47:71–95.
13. Saez-Briones, P., M. Krauss, M. Dreger, A. Herrmann, V. I. Tsetlin, et al. 1999. How do acetylcholine receptor ligands reach their binding sites? *Eur. J. Biochem.* 265:902–910.
14. Sunshine, C., and M. G. McNamee. 1992. Lipid modulation of nicotinic acetylcholine receptor function: the role of neutral and negatively charged lipids. *Biochim. Biophys. Acta.* 1108:240–246.
15. De Planque, M. R., D. T. Rijkers, J. I. Fletcher, R. M. Liskamp, and F. Separovic. 2004. The $\alpha$M1 segment of the nicotinic acetylcholine receptor exhibits conformational flexibility in a membrane environment. *Biochim. Biophys. Acta.* 1665:40–47.
16. De Planque, M. R., D. T. Rijkers, R. M. Liskamp, and F. Separovic. 2004. The $\alpha$M1 transmembrane segment of the nicotinic acetylcholine receptor interacts strongly with model membranes. *Magn. Reson. Chem.* 42:148–154.
17. Miwa, J. M., I. Ibanez-Tallon, G. W. Crabtree, R. Sanchez, A. Sali, et al. 1999. lynx1, an endogenous toxin-like modulator of nicotinic acetylcholine receptors in the mammalian CNS. *Neuron.* 23:105–114.
18. Young, H. S., L. G. Herbette, and V. Skita. 2003. $\alpha$-Bungarotoxin binding to acetylcholine receptor membranes studied by low angle X-ray diffraction. *Biophys. J.* 85:943–953.
19. Dubovskii, P. V., D. M. Lesovoy, M. A. Dubinnyi, A. G. Konshina, Y. N. Utkin, et al. 2005. Interaction of three-finger toxins with phospholipid membranes: comparison of S- and P-type cytotoxins. *Biochem. J.* 387:807–815.
20. Dubinnyi, M. A., D. M. Lesovoy, P. V. Dubovskii, V. V. Chupin, and A. S. Arseniev. 2006. Modeling of 31P-NMR spectra of magnetically oriented phospholipid liposomes: a new analytical solution. *Solid State Nucl. Magn. Reson.* 29:305–311.
21. Piotto, M., V. Saudek, and V. Sklenar. 1992. Gradient-tailored excitation for single-quantum NMR spectroscopy of aqueous solutions. *J. Biomol. NMR.* 2:661–665.
22. Zhang, O., L. E. Kay, J. P. Olivier, and J. D. Forman-Kay. 1994. Backbone 1H and 15N resonance assignments of the N-terminal SH3 domain of drk in folded and unfolded states using enhanced-sensitivity pulsed field gradient NMR techniques. *J. Biomol. NMR.* 4:845–858.
23. Bocharov, E. V., E. N. Lyukmanova, Y. S. Ermolyuk, A. A. Schulga, K. A. Pluzhnikov, et al. 2003. Resonance assignment of 13C/15N-labeled snake neurotoxin II from *Naja oxiana*. *Appl. Magn. Reson.* 24:247–254.
24. Berendsen, H. J. C., D. van der Spoel, and R. van Drunen. 1995. GROMACS. *Comput. Phys. Commun.* 91:43–56.
25. Schiebler, W., and F. Hucho. 1978. Membranes rich in acetylcholine receptor: characterization and reconstitution to excitable membranes from exogenous lipids. *Eur. J. Biochem.* 85:55–63.
26. Watts, A. 1998. Solid-state NMR approaches for studying the interaction of peptides and proteins with membranes. *Biochim. Biophys. Acta.* 1376:297–318.
27. Saito, H., I. Ando, and A. Naito. 2006. $^{31}$P NMR. *In* Solid State NMR Spectroscopy for Biopolymers. H. Saito, I. Ando, and A. Naito, editors. Springer, Dordrecht, The Netherlands. 59–68.
28. Dufourc, E. J., C. Mayer, J. Stohrer, G. Althoff, and G. Kothe. 1992. Dynamics of phosphate head groups in biomembranes. Comprehensive analysis using phosphorus-31 nuclear magnetic resonance lineshape and relaxation time measurements. *Biophys. J.* 61:42–57.
29. Qiu, X., P. A. Mirau, and C. Pidgeon. 1993. Magnetically induced orientation of phosphatidylcholine membranes. *Biochim. Biophys. Acta.* 1147:59–72.
30. Dubovskii, P. V., D. M. Lesovoy, M. A. Dubinnyi, Y. N. Utkin, and A. S. Arseniev. 2003. Interaction of the P-type cardiotoxin with phospholipid membranes. *Eur. J. Biochem.* 270:2038–2046.
31. Matsuo, H., K. J. Walters, K. Teruya, T. Tanaka, G. T. Gassner, et al. 1999. Identification by NMR spectroscopy of residues at contact surface in large, slowly exchanging macromolecular complexes. *J. Am. Chem. Soc.* 121:9903–9904.
32. Korchuganov, D. S., S. B. Nolde, M. Y. Reibarkh, V. Y. Orekhov, A. A. Schulga, et al. 2001. NMR study of monomer-dimer equilibrium of barstar in solution. *J. Am. Chem. Soc.* 123:2068–2069.
33. Petrache, H. I., S. Tristram-Nagle, K. Gawrisch, D. Harries, V. A. Parsegian, et al. 2004. Structure and fluctuations of charged phosphatidylserine bilayers in the absence of salt. *Biophys. J.* 86:1574–1586.
34. Unwin, N. 2005. Refined structure of the nicotinic acetylcholine receptor at 4A resolution. *J. Mol. Biol.* 346:967–989.
35. Kovacic, P., R. S. Pozos, and C. D. Draskovich. 2007. Unifying electrostatic mechanism for receptor-ligand activity. *J. Recept. Signal Transduct. Res.* 27:411–431.
36. Sargent, D. F., and R. Schwyzer. 1986. Membrane lipid phase as catalyst for peptide-receptor interactions. *Proc. Natl. Acad. Sci. USA.* 83:5774–5778.
37. Antil, S., D. Servent, and A. Menez. 1999. Variability among the sites by which curaremimetic toxins bind to *Torpedo* acetylcholine receptor, as revealed by identification of the functional residues of $\alpha$-cobratoxin. *J. Biol. Chem.* 274:34851–34858.
38. Ducancel, F., K. Merienne, C. Fromen-Romano, O. Tremeau, L. Pillet, et al. 1996. Mimicry between receptors and antibodies. Identification of snake toxin determinants recognized by the acetylcholine receptor and an acetylcholine receptor-mimicking monoclonal antibody. *J. Biol. Chem.* 271:31345–31353.
39. Samson, A. O., and M. Levitt. 2008. Inhibition mechanism of the acetylcholine receptor by $\alpha$-neurotoxins as revealed by normal-mode dynamics. *Biochemistry.* 47:4065–4070.
40. Tsetlin, V. I., E. Karlsson, Y. Utkin, K. A. Pluzhnikov, A. S. Arseniev, et al. 1982. Interaction surfaces of neurotoxins and acetylcholine receptor. *Toxicon.* 20:83–93.
41. Honig, B., and A. Nicholls. 1995. Classical electrostatics in biology and chemistry. *Science.* 268:1144–1149.